COBEM 2023 27TH INTERNATIONAL CONGRESS OF MECHANICAL ENGENEERING

ABCM Brazilian Society of Mechanical Sciences and Engineering
27th ABCM International Congress of Mechanical Engineering
December 04-08, 2023, Florianópolis-SC, Brazil

COB-2023-0889
ACTIVATION OF BONE MASS MAINTENANCE THROUGH INTRAMEDULLARY NAIL DYNAMIZATION

José Renato de Oliveira e Silva Neto[1]
Paulo Pedro Kenedi[1,2]
[1]PPEMM - Post-Graduate Program in Mechanical Engineering and Materials Technology – CEFET/RJ, Av. Maracanã, 229, RJ,
[2]CCGMEC – Mechanical Engineering Department - CEFET/RJ, Av. Maracanã, 229, RJ, Brazil
jose.neto@aluno.cefet-rj.br
paulo.kenedi@cefet-rj.br

Rodrigo Ribeiro Pinho Rodarte
National Institute of Traumatology and Orthopedics - INTO, Av. Brazil, 500, RJ, Brazil
rrodarte@into.saude.gov.br

Lucas Lisbôa Vignoli
Center of Technology and Application of Composite Materials, Federal University of Rio de Janeiro, Macaé, RJ, Brazil
lucas.lvig@gmail.com

Abstract. *Diaphyseal fractures are very common in the elderly and may be related to low bone mineral density. Mechanical factors such as the magnitude of bone strain induced by load, and the number of daily load cycles are important in modeling and maintaining bone mass. However, the action of these mechanisms may slow down in elderly adults, if it is considered factors such as physical limitations or lack of ability to physical activity. Although the intramedullary nail is quite effective in stabilizing fractures, blocking this device can lead to an increase in difficulty in maintaining bone mass. The ANSYS finite element software was used to verify the levels of strain experienced by the diaphyseal cortex of a post-healing human femur bone through the actuation of a simple loading case. Three different materials of locked intramedullary nails were tested, dynamized or not. A linear regression curve proposed by Qin was used to combine strain peaks and the number of daily load cycles, comparatively, to estimate the combinations that could maintain bone mass. It was shown that the dynamization of a low-stiffness nail has the potential to reduce to half the number of daily load cycles necessary to maintain bone mass. These results may help in the decision to maintain, dynamize or even remove the nail after fracture stabilization.*

Keywords: *intramedullary nail, FE Analysis, strain shielding, bone modeling, bone mass maintenance.*

1. INTRODUCTION

The knowledge about bone tissues, regarding formation process, remodeling, healing, or fracture stabilization experienced good progress in the last two decades. After a shaft fracture, an inflammation response starts with the local recruitment of mesenchymal stem cells responsible for proliferating, differentiating, and forming a bone callus. Later, a revascularization process, neoangiogenesis, cartilage mineralization, and resorption translation are carried out. The resulting fracture site is remodeled through the balance of the hard callus translation resorption done by osteoclasts, and the deposition of lamellar bone performed by osteoblasts, (Marsell1 and Einhorn, 2011). This conceptual framework is known as the Diamond Concept. It is used as a biological tool for healing fracture translation, also, has also been quite useful in stabilization therapies in cases of non-union of fractures, including cases of comorbidity (Andrzejowski and Giannoudis, 2019). Moreover, mechanobiological modeling has been studied to understand the interaction between biological and mechanical factors in bone healing (Ghiasi *et al*., 2017).

The most efficient device used in fracture stabilization is the locked intramedullary nailing (IN). It was implemented by a German orthopedic surgeon, Gerhard Kuntscher, to stabilize fractures in American pilots during the Second war (Glatt *et al*., 2017). The reduced stabilization time and low risk of complications have consolidated the utilization of this technique, although some setbacks have been related to the strain shielding caused by the device (Allen *et al*., 2008). This phenomenon can be mitigated by using low-stiffness materials, such as composite laminates, minimizing bone loss at the fracture site (Samiezadeh *et al*., 2015). Several authors approach strain shielding with a focus on bone resorption and the consequent device loosening results (Cilla *et al*., 2017). A clinical practice largely suggested by many authors, in case of delayed union and non-union of diaphyseal fractures, is the utilization of the *IN* dynamization technique, which can be

more advantageous than other techniques, considering the time and cost savings. By removing one of the translation locking screws, whether proximal or distal, the mechanical stimulation of the fracture site can be enhanced. The *IN* dynamization analysis showed an optimal callus-to-diaphysis ratio, allowing a 93% rate of union, for the cases studied by (Vaughn *et al*., 2016). Nevertheless, there are uncertainties about the influence of dynamization after the healing process has ended. An experimental study involving animal models concluded that late dynamization might have a beneficial effect on bone (Claes *et al*., 2009). Although the acceleration of the healing process has been massively studied, the load share impacts after healing are still less investigated. The interlocking nailing system is normally not removed after healing, maintaining the load share between bone and nailing. Therefore, this phenomenon should also be observed with a focus on post-healing bone quality, with a static locking pin removal being an option after healing has ended, as a less invasive procedure.

The present study aims to assess the possible impact of the load share between bone and *IN*, after stabilization of a fracture. Is the effect of the load share between bone and nailing in bone modeling (Bm) and bone remodeling (Br) mechanisms after post-healing significant? According to the mechanistic hypothesis, strains can enhance bone healing (Frost, 2003). The adaptive process of architectural and material adjustment carried out by remodeling is partly responsible for the formation and maintenance of bone functionality (Tyrovola and Odont, 2015). In homeostasis, constant changes in the remodeling cycle support the repair of microdamage and the replacement of dead cells with new tissue (Ozcivici *et al*., 2010). An imbalance between the formation and reabsorption phases can lead to fractures or even a decrease in bone density, known as osteoporosis. *Br* and *Bm* need to work together whenever a bone repair process is required, either by architectural and material adjustment or even when a device is integrated into the bone tissue, (García-Aznar *et al*., 2021). The bone adaptation cannot be explained as simply a consequence of Wolff's Law, if there is no balance between *Bm* and *Br*, other joint structures may be affected (Teichtahl *et al*., 2015).

A translation of studies in animal models to human ones was used to estimate the limit for bone mass maintenance (BMM), through the product of strain magnitude versus number of daily load cycles (DLC). A nonlinear regression equation with a slope of approximately 4-5 to fit modeling data from live animals, as well as observations made in human studies, has been suggested (Qin *et al*., 1998). A randomized study in rats reinforced the hypothesis that an increase in the magnitude of strain reduces the minimum *DLC* required by the bone formation mechanism. (Cullen *et al.*, 2001). It was considered that 95% of the mechanosensitivity process started with a strain rate of just 40 *DLC* under approximately 2000 με in compression of magnitude (Hart *et al*., 2017). Such magnitude of strain in human bone is not easily achieved by a simple walk. An external loading regression model observed an increase in bone mass for a strain rate of 1,000 με with just 100 *DLC* at a frequency of 1 Hz (Rubin and Lanyon, 1985). Strain of high magnitude in a short period combined with rest intervals proved to be more effective in osteogenic stimulation if compared to more prolonged loading protocols (Burr *et al*., 2002). Due to the limitations of in vivo models to assess the levels of strain experienced by bone tissue, open-source musculoskeletal models have been used to better estimate hip contact forces derived from a set of muscle forces involved in walking and stair climbing loading protocols. The results were close to those measured in vivo models with instrumented prostheses. (Modenese *et al*., 2011). However, the usual *BMM* mechanism may be not sufficient for elderly adults if we consider factors such as moderate capacity and availability for training at high magnitudes of strain. Therefore, the dynamization process of the *IN*, after fracture stabilization, is being evaluated as an option to eliminate the strain shielding of the bone/nailing set, contributing to a better quality of life.

2. METHODS AND MATERIALS

A given moment of gait protocol, through the utilization of a simplified model of muscle selection, is used to propose numerical model (NM) loading of the bone and *IN* set, as in (Duda *et al*., 1998). It considers three different types of nailing materials, with or without *IN* device dynamization. Through the utilization of the maximum compressive longitudinal peaks found in *NM* are used in the *BMM* curve to estimate the respective minimum *DLC* required.

2.1 The Numerical Model – Strain Estimation

A three-dimensional model, which included cortical and cancellous bone, *IN,* and the interlocking system, was developed using the finite element (FE) software ANSYS 16 Workbench. The analyses involve evaluating the effect of a simple loading case. It is composed of static loading acting on the proximal femur under a given moment of gait protocol. The simple loading case uses an equivalent of seventy kilograms on joint reaction and two main muscle forces, in addition to locking the distal region (Vignoli and Kenedi, 2016) as shown in Fig 1. a. The proximal locking screw has 68 mm in length and 6 mm in outer diameter. The distal locking screws were both 36 mm in length and 4.5 mm in outer diameter. Fig. 2 shows the screw details. Fig. 1.b shows the nine cross sections of the femur/IN set analysed in this work. Note the quite significative cross-section shape variation in the function of each vertical position.

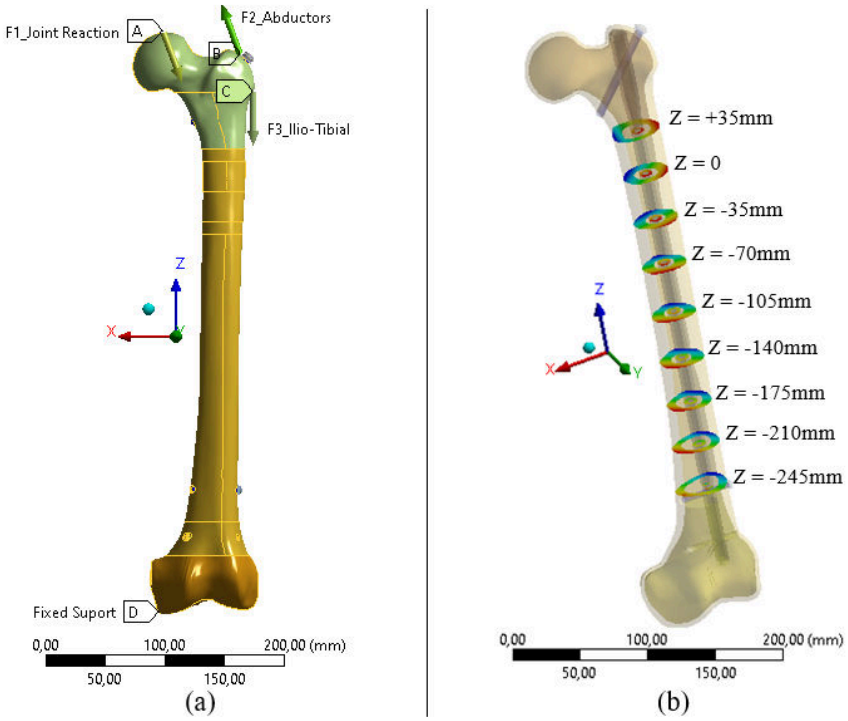

Figure 1. (a) Numerical Model with the simple loading case in the femur/IN set and (b) Details of the nine cross sections of the femur/IN set.

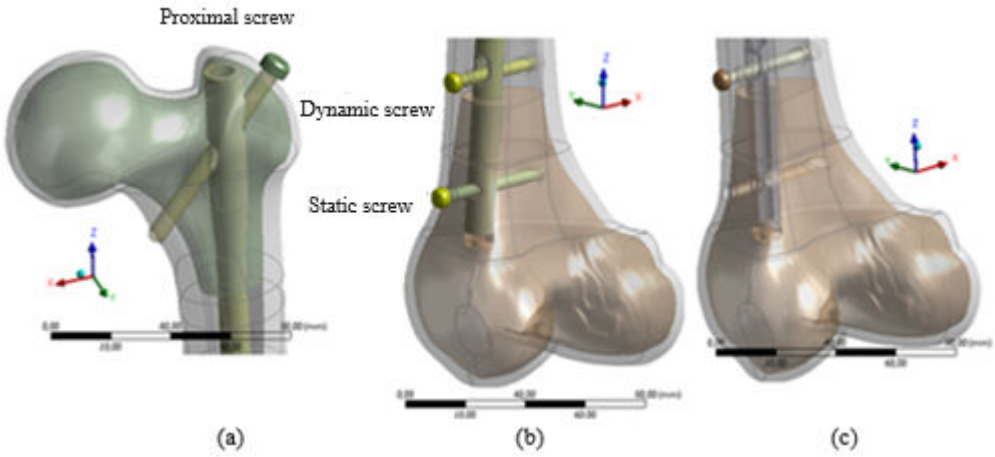

Figure 2. (a) Proximal Screw Detail, (b) Distal end with Locked Nailing, and (c) Dynamized Nailing.

In Table 1 the values of load forces, under a given moment of gait protocol, are presented. The *IN* was modeled with a length of 410 mm, 10 mm in outer diameter, and 2.5 mm in wall thickness.

Table 1. Applied Forces.

		F_x (N)	F_y (N)	F_z (N)	F_r (N)
F1	Joint Reaction	-265.5	-32.5	-700	749.36
F2	Abductors	107.5	0	290	309.28
F3	Ilio-Tibial	0	0	-300	300

It was assumed that the simple loading case should produce differences in strains superior by 26% if compared to a more complex loading case with all thigh muscles involved (Duda *et al*., 1998). The analyses considered three different cases (*A*, *B*, *C*) of materials for locked *IN* and a fourth case, named *D*, as case C for dynamized *IN*. Table 2 shows the four different cases studied.

Table 2. The four different cases.

Nail case	*IN* Material	
A	Stainless Steel (StSt)	Locked
B	Titanium (Ti) (1)	Locked
C	Composite CF/Epoxy	Locked
D	Composite CF/Epoxi (*)	Dynamized

(1) also for locking screws.

As shown in (Vignoli and Kenedi, 2016) the level of anisotropy plays a role in bone strains, thus the *FE* analysis considered the following constitutive relations: linear, elastic, and orthotropic behavior were attributed to the cortical bone; and linear, elastic, and isotropic behavior were attributed for cancellous bone and nailing. For the composite nailing the effective elastic properties of the laminate were obtained by the asymptotic homogenization technique (Samiezadeh *et al.*, 2015).

All locking screws were simplified as cylinders. Since the model was completely balanced, the rigid body motions were restricted by fixing the three-axis displacement for the cortical distal end. Table 3 shows the elastic mechanical properties of bone, nailing, and screws.

Table 3. Elastic Mechanical Properties.

Material	Young's Modulus E (GPa)			Poisson's Ratio ν		
Cortical Bone (1)	E_1	E_2	E_3	xy	yz	xz
	12	13.4	20	0.376	0.234	0.222
Cancellous Bone	0.155			0.3		
StSt (ISO 5832-9)	191.3			0.3		
Ti (Ti6Al4V)(2)	113.8			0.342		
Composite CF/Epoxy	x	y	z	xy	yz	xz
	9.89	33.922	39.169	0.0661	0.427	0.0501

(1) (Vignoli and Kenedi, 2016) (2) for CASE B *NI* and all screws

Fig. 3 shows the meshing details. A 40 mm radius sphere of influence was used to reach a 1.5 mm mesh for bone and nailing around the distal screws. It used 214448 solid elements (SOLID185, SOLID186, and SOLID187) and contact elements (CONTA174 and TARGE170), as well as 349395 nodes. All contact surfaces between bone, nail, and locking screws were considered as BONDED, with the use of Model Predictive Control (MPC) formulation. Just for the dynamized nail (Case D), the nailing-dynamic screw contact was set as FRICTIONAL with a 0.263 friction coefficient.

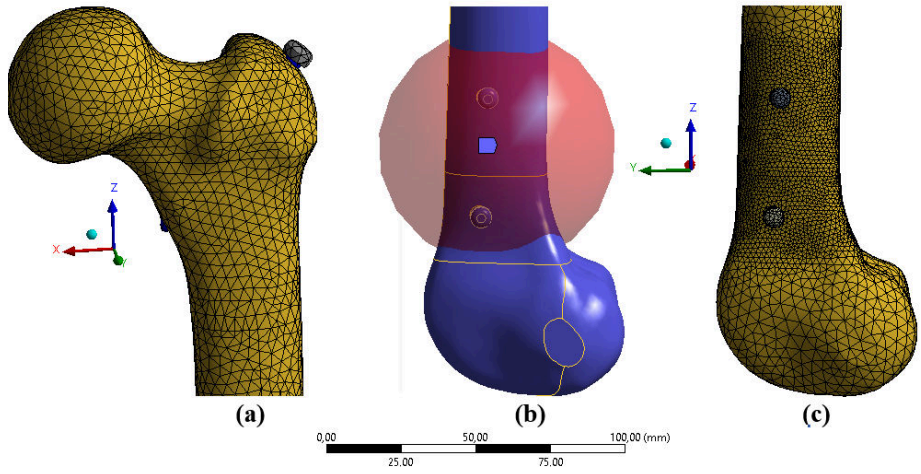

Figure 3. Meshing Details on Cortical Bone: (a) Proximal, (b) Sphere of influence, and (c) Distal.

Note that the aim of the utilization of the Sphere of influence was to refine the mesh near tiny details such as the screw holes.

2.2 The BMM model – Load Cycles Estimation

To implement the *BMM* estimation model, it was considered that the strain threshold required to maintain the bone mass could be expressed by the nonlinear regression equation proposed by (Qin *et al*., 1998), where *DLC* is the daily load cycles and ε is the longitudinal strain magnitude required for *BMM*. Equation (1) is used to generate the *BMM* curve. Equation (2) is the equivalent of equation (1), used to estimate the *DLC* value in function of the *FE* strain results.

$$\varepsilon = 10^{2.28} \cdot (5.6 - \log_{10}(DLC))^{1.5} \quad (1)$$

$$DLC = 10^{\left(5.6-\left(\frac{\varepsilon}{10^{2.28}}\right)^{1/1.5}\right)} \quad (2)$$

Note that the equation proposed by (Qin *et al*., 1998) is based on limited experimental results. Both equations (1) and (2) must be used with caution. The results of equation (2) application were used only in a comparative way, in conjunction with *FE* results, to indicate which of the four cases presented in the paper (cases *A*, *B*, *C,* or *D*) has the best performance. Also, variables such as gait frequency and effort rate were not considered. Attenuating the minimum amount of *DLC* to guarantee *BMM* or avoiding the limited range of reabsorption (MESr) seems to be very advantageous for those whose ability or availability to practice physical activity is considered a limiting factor, as is the case of the elderly.

3. RESULTS AND DISCUSSIONS

In section 2, the *FE* model was detailed, with the geometry, forces, boundary conditions, and mechanical properties. In this section, the longitudinal bone strains output generated by the *FE* are made available, for the forces presented in Table 1. Fig. 4 shows the periosteum longitudinal strains for cases *C* and *D*.

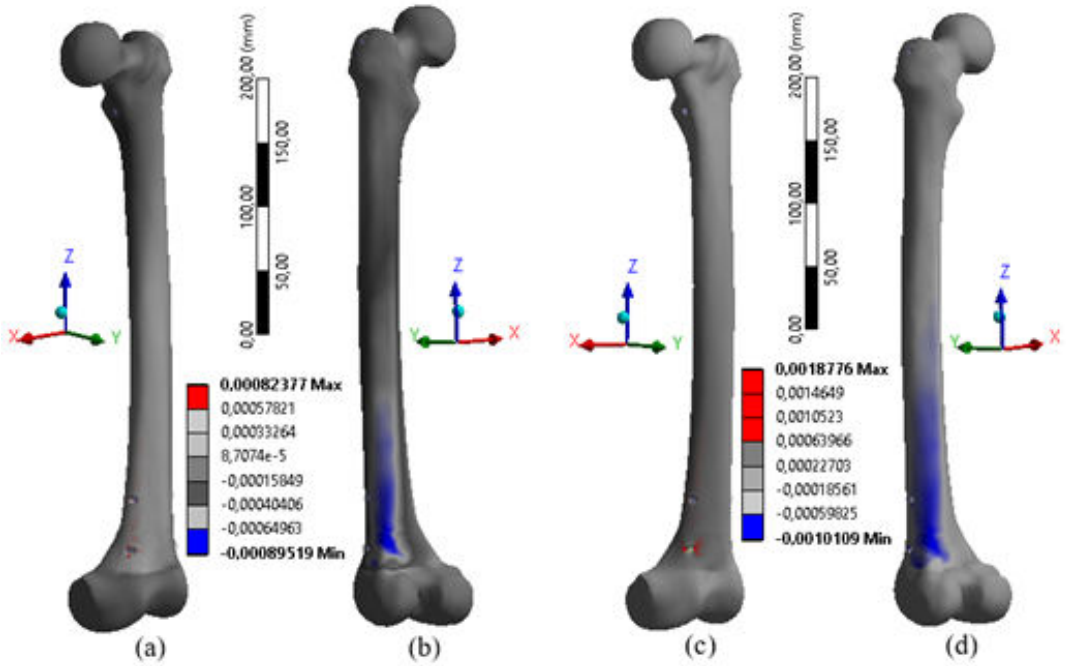

Figure 4. Periosteum Longitudinal Strains with simple loading case: (a) CASE *C* (meso-anterior), (b) CASE *C* (lateral-posterior), (c) CASE *D* (meso-anterior), and (d) CASE *D* (lateral-posterior).

The maximum longitudinal strain (MLS) around the holes of the locking screws were isolated and discarded, as points of numerical model distortion. These higher values appear in red, and are almost imperceptible, on the screw hole edge as apparent in Fig. 4.a and 4. c. The gray scale represents the intermediate tensile and compressive strains, and the blue colour indicates the maximum compressive strains.

Table 4 summarizes the *MLS*, located in the periosteum, for each nail case (*A*, *B*, *C,* and *D*), for the simple loading case.

Table 4. Longitudinal Compressive Strain in the Periosteum.

Nail case	Simple loading case *MLS* (με)	DLC(*)/distance (km)
A (locked StSt nail)	-825	878/1.3
B (locked Ti nail)	-887	649/1.0
C (locked composite nail)	-895	836/1.2
D (dynamized composite nail)	-1011	361/0.5

(*) 1 Cycle = 2 steps = 1,46m

Note that the *MLS* results for cases *A*, *B,* and *C*, of Table 4, are quite similar for the simple loading case. Only for case *D,* there is a significant difference in *MLS* results, with obvious consequences in the *DLC* results. Case *D* requires less than half the daily distance (0.5 km) compared to case *A* (1.3 km). In this case, the maximum magnitude of strain achieved in the bone model with dynamized *IN* was shown to be around 13% higher than the model with locked *IN*.

In Fig. 5, the compressive peaks were plotted on the *BMM* curve, for the four cases studied, considering the specific moment of the gait protocol. It is a graphical representation of the results shown in Table 4. Note that the Frost mechanotransduction windows are superimposed (Frost, 2003) in Fig. 5.

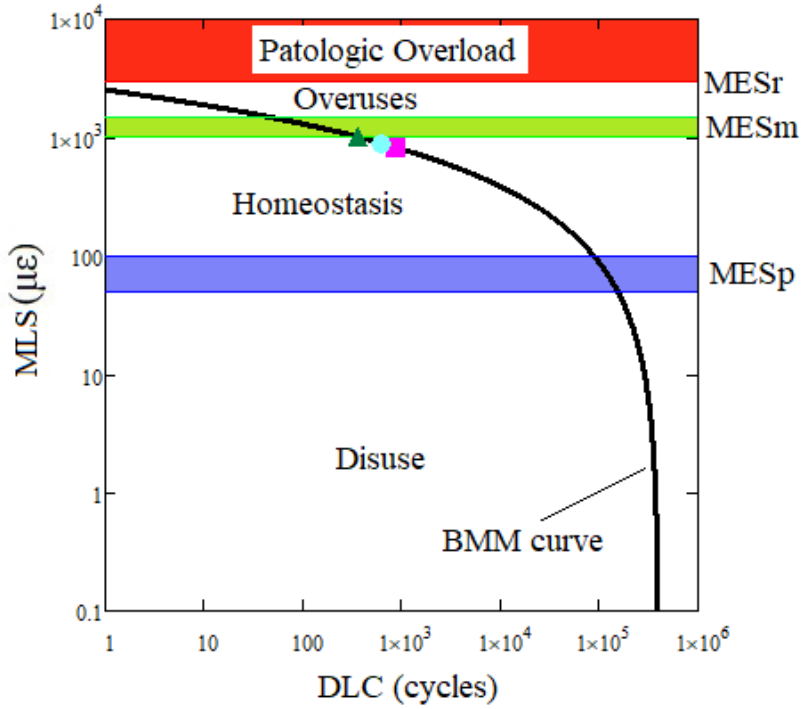

Figure 5. *MLS* vs *DLC* graphic for simple loading case. CASE *A* – magenta squares, CASE *B* – orange rhombus, CASE *C* – cyan circles, and CASE *D* – olive triangles. The Frost mechanotransduction windows are superimposed (Frost, 2003).

Analysing Fig. 5, it is apparent that *A*, *B,* and *C* cases have a very close performance. Case *D* has a little better performance, not very apparent because of the logarithm scale of the coordinate axes. The generated strains in all cases are in bone and nailing elastic range. Nevertheless, the dynamization process shown in case *D* produces a significant reduction in walking necessity, when compared with the other three cases, cutting by half the necessary walking distance. Note that depending on the loading protocol, muscle groups involved, and the gait instant, a given bone section may or may not activate by bone modeling.

Fig. 6 shows, at cross-section for Z = -245mm (see Fig.1.b), the Cortical Bone Longitudinal Strain for the simple loading case: (a) CASE *A* and (b) CASE *D*.

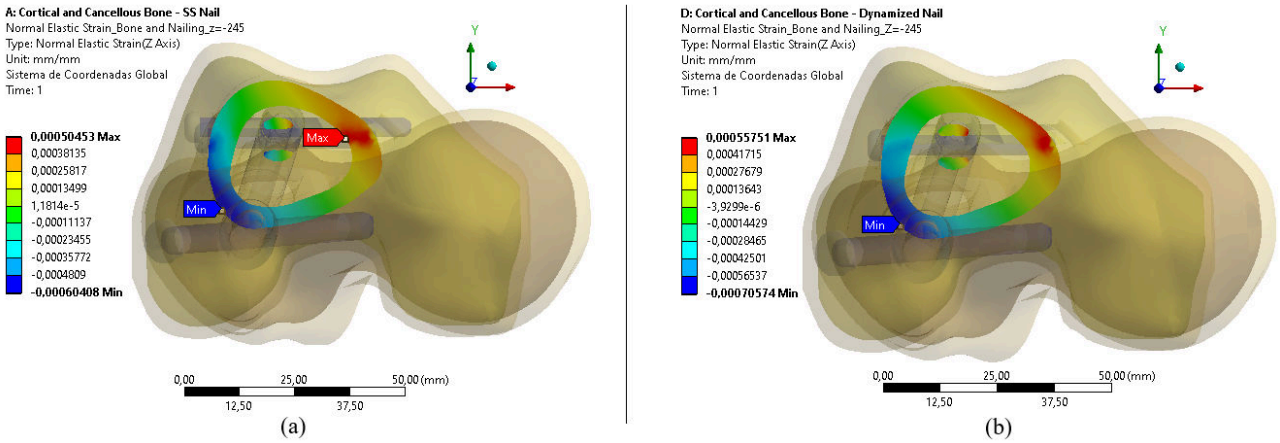

Figure 6. Cross-Section (Z = -245mm) – Cortical Bone Longitudinal Strain for the simple loading case: (a) CASE *A* and (b) CASE *D*.

Note the significative difference in compressive strains, represented by the blue color, obtained by the dynamization of the nailing case *D*.

4. CONCLUSIONS

The strain magnitude that bones cross sections are submitted is a mechanical factor of fundamental importance in the mechanism of mechanotransduction. So, the utilization of low-stiffness materials by the *IN* seems to be the right choice, in the way that the *NI* shares less load from the bone/nail set. An even better result can be achieved, in the post-healing phase, by implementing the dynamization procedure on a low-stiffness *IN*. Preliminary results show that it is possible to cut up to half of the *DCL* to achieve the *BMM* by completing the *IN* dynamization. This is a significant result, considering, for instance, the limitations of elderly people. In short, the quantification of the bone strain by the *FE* model, in conjunction with the utilization of a *BMM* estimation model, showed the advantage of the implementation of the *IN* dynamization process, for attenuating the need for excessive *DLC* to achieve *BMM*.

5. ACKNOWLEDGEMENTS

José R. O. S. Neto is grateful for the scholarship granted by CAPES.

6. REFERENCES

Allen, J. C., Jr., Lindsey, R. W., Hipp, J. A., Gugala, Z., Rianon, N., and Leblanc, A., 2008, The Effect of Retained Intramedullary Nails on Tibial Bone Mineral Density. Clin. Biomech. (Bristol, Avon), Vol.23(6), pp. 839–843. https://doi.org/10.1016/j.clinbiomech.2008.02.003.

Andrzejowski, P. and Giannoudis, P. V. 2019, The 'diamond concept' for long bone non-union management. Journal of Orthopaedics and Traumatology, Vol.20(1), pp.1-13. https://doi.org/10.1186/s10195-019-0528-0.

Burr, D. B., Robling, A. G., Turner, C. H., 2002, Effects of Biomechanical Stress on Bones in Animals. Indiana University School of Medicine, Indianapolis, IN, USA, Vol. 30(5), pp.781-786.

Cilla, M., Checa, S. and Duda, G. N., 2017, Strain shielding inspired re-design of proximal femoral stems for total hip arthroplasty. Journal of Orthopaedic Research, Vol. 35(11), pp.2534–2544. https://doi.org/10.1002/jor.23540.

Claes, L., Blakytny, R., Melanie Göckelmann, Schoen, M., Ignatius, A. and Willie, B., 2009, Early dynamization by reduced fixation stiffness does not improve fracture healing in a rat femoral osteotomy model. Journal of Orthopaedic Research, Vol. 27(1), pp. 22–27. https://doi.org/10.1002/jor.20712.

Cullen, D. M., Smith, R. T. and Akhter, M. P., 2001, Bone-loading response varies with strain magnitude and cycle number. Journal of Applied Physiology, Vol. 91(5), pp.1971–1976. https://doi.org/10.1152/jappl.2001.91.5.1971.

Duda, G. N., Heller, M., Albinger, J., Schulz, O., Schneider, E., and Claes, L., 1998, Influence of muscle forces on femoral strain distribution. Journal of Biomechanics, Vol. 31(9), pp.841–846. https://doi.org/10.1016/S0021-9290(98)00080-3.

Frost, H. M. 2003. Bone's Mechanostat: A 2003 Update. Anatomical Record - Part A Discoveries in Molecular, Cellular,

and Evolutionary Biology, Vol. 275 (2), pp.1081–1101. https://doi.org/ 10.1002/ar.a.10119.
García-Aznar, J. M., Nasello, G., Hervas-Raluy, S., Pérez, M. Á. and Gómez-Benito, M. J., 2021, Multiscale modeling of bone tissue mechanobiology. Bone, Vol. 151(June). https://doi.org/10.1016/j.bone.2021.116032.
Ghiasi, M. S., Chen, J., Vaziri, A., Rodriguez, E. K. and Nazarian, A., 2017, Bone fracture healing in mechanobiological modeling: A review of principles and methods. Bone Reports, Vol. 6, pp. 87–100. https://doi.org/10.1016/j.bonr.2017.03.002.
Glatt, V., Evans, C. H. and Tetsworth, K., 2017, A concert between biology and biomechanics: The influence of the mechanical environment on bone healing. Frontiers in Physiology, Vol. 7 (JAN). https://doi.org/10.3389/fphys.2016.00678.
Hart, N. H., Nimphius, S., Rantalainen, T., Ireland, A., Siafarikas, A. and Newton, R. U., 2017, Mechanical basis of bone strength: Influence of bone material, bone structure, and muscle action. Journal of Musculoskeletal Neuronal Interactions, Vol. 17(3), pp. 114–139.
Qin, Y. X., Rubin, C. T. and McLeod, K. J., 1998, The nonlinear dependence of loading intensity and cycle number in the maintenance of bone mass and morphology. Journal of Orthopaedic Research, Vol. 16(4), pp. 482–489. https://doi.org/10.1002/jor.1100160414.
Modenese, L., Phillips, A. T.M., Bull, A. M.J., 2011, An open source lower limb model: Hip joint validation. Journal of Biomechanics. Vol. 44(12), pp. 2185-2193. http://dx.doi.org/10.1016/j.jbiomech.2011.06.019.
Marsell, R. and Einhorn, T.A., 2011, The Biology of Fracture Healing. National Institutes of Health, Vol. 42(6), pp.551–555. https://doi.org/10.1016/j.injury.2011.03.031.
Ozcivici et al., 2010, Mechanical signals as anabolic agents in bone. Nat Rev Rheumatol. Vol. 6(1), pp.50–59. https://doi.org/10.1038/nrrheum.2009.239.
Rubin, C.T. and Lanyon, L.E., 1985, Regulation of the Bone Mass by Mechanical Strain Magnitude. Calcified Tissue International, Vol. 37, pp.411-417. https://doi.org/10.1007/BF02553711.
Samiezadeh, S., Avval, P. T., Fawaz, Z. and Bougherara, H., 2015, An Effective Approach for Optimization of a Composite Intramedullary Nail for Treating Femoral Shaft Fractures. Journal of Biomechanical Engineering, Vol. 137(12). pp. 121001-1 - 121001-9. https://doi.org/10.1115/1.4031766.
Teichtahl, A. J., Wluka, A. E., Wijethilake, P., Wang, Y., Ghasem-Zadeh, A. and Cicuttini, F. M., 2015, Wolff's law in action: A mechanism for early knee osteoarthritis. Arthritis Research and Therapy, Vol. 17(1), pp. 1–9. https://doi.org/10.1186/s13075-015-0738-7.
Tyrovola, J. B. and Odont, X. X., 2015, The "mechanistic Theory" of Frost and the OPG/RANKL/RANK System. Journal of Cellular Biochemistry, Vol. 116(12), pp. 2724–2729. https://doi.org/10.1002/jcb.25265.
Vaughn, J., Gotha, H., Cohen, E., Fantry, A. J., Feller, R. J., Van Meter, J., Hayda, R. and Born, C. T., 2016, Nail dynamization for delayed union and nonunion in femur and tibia fractures. Orthopedics, Vol. 39(6), pp. e1117–e1123. https://doi.org/10.3928/01477447-20160819-01.
Vignoli, L. L., & Kenedi, P. P., 2016, Bone anisotropy – Analytical and finite element analysis. Latin American Journal of Solids and Structures, Vol.13(1), pp. 51–72. https://doi.org/10.1590/1679-78251814.

7. RESPONSIBILITY NOTICE

The authors are the only ones responsible for the printed material included in this paper.